Electronic Supplementary Material (ESI) for Analytical Methods.

Supplementary Information

Low-cost voltammetric sensor based on multi-walled carbon nanotubes for highly sensitive and accurate determination of nanomolar level of anticancer drug Ribociclib in bulk and biological fluids

Wiem Bouali [a b], ***Nevin Erk*** [a], ***Asena Ayse Genc*** [a b]

[a] Ankara University, Faculty of Pharmacy, Department of Analytical Chemistry, 06560 Ankara, Turkey

[b] Ankara University, The graduate school of the health sciences, 06110 Ankara, Turkey

Email corresponding author: erk@pharmacy.ankara.edu.tr

wbouali@ankara.edu.tr

Materials and Reagents

In this study, Glucose (99.5 %), L-arginine (98.0 %), L-methionine, sodium hydroxide, potassium hexacyanoferrate (III) ($K_3Fe(CN)_6$, 99.5 %), hydrochloric acid, sodium Acetate, ascorbic acid, uric acid (99.0 %), acetic acid, potassium chloride, sodium phosphate, sodium sulfate, potassium chloride, sodium sulfate, were purchased from Sigma Aldrich Co. (https://www.sigmaaldrich.com, Germany). Multiwalled carbon nanotubes (CAS Number: 308068-56-6) were obtained from Merck Company (Darmstadt, Germany). Britton-Robinson buffer was made of boric acid, phosphoric acid, potassium chloride, and acetic acid solutions. Ribociclib was obtained from selleckchem.com. The stock solution of RIBO was prepared in methanol: water (1:1). Human plasma samples were also acquired from Sera-Flex Inc. All chemical compounds were analytical grade and used without additional refinement.

Apparatus

Voltammetric experiments were carried out using AUTO LAB system with PGSTAT204 electrochemical workstation (Metrohm Inc., Switzerland) with a glassy carbon electrode system in a one-compartment of 10 mL electrochemical cell. All electrochemical measurements were performed at 25 ˚C unless otherwise specified.

The Randles-Sevcik equation:

$$I = (2.69 \times 10^5)\, n^{\frac{3}{2}}\, A\, D^{\frac{1}{2}}\, v^{\frac{1}{2}}\, C_0 \qquad (S1)$$

I is the anodic or cathodic peak current, A represents the electrode area in cm^2, D shows the diffusion coefficient (cm^2/s), n is the number of electrodes (n = 1), *v* exhibits the potential scan rate (V/s), and C_0 is the concentration (mol/cm^3).

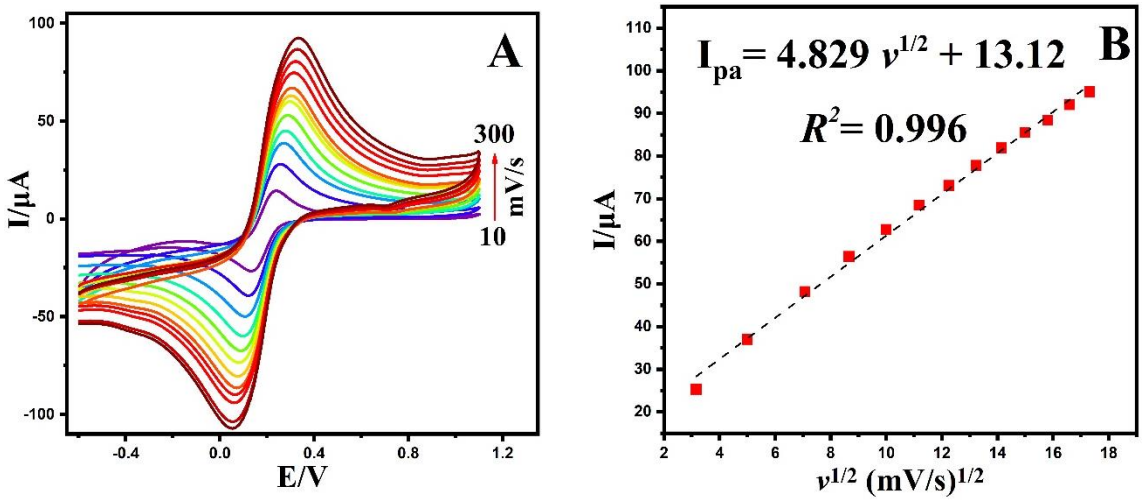

Figure S1. The recorded CV curves at various scan rates in the presence of 5.0 mM $[Fe(CN)_6]^{3-/4-}$ containing 0.1 M KCl (A), and the relationship between Ipa vs. $v^{1/2}$ (B), on bare the MWCNTs/GCE.

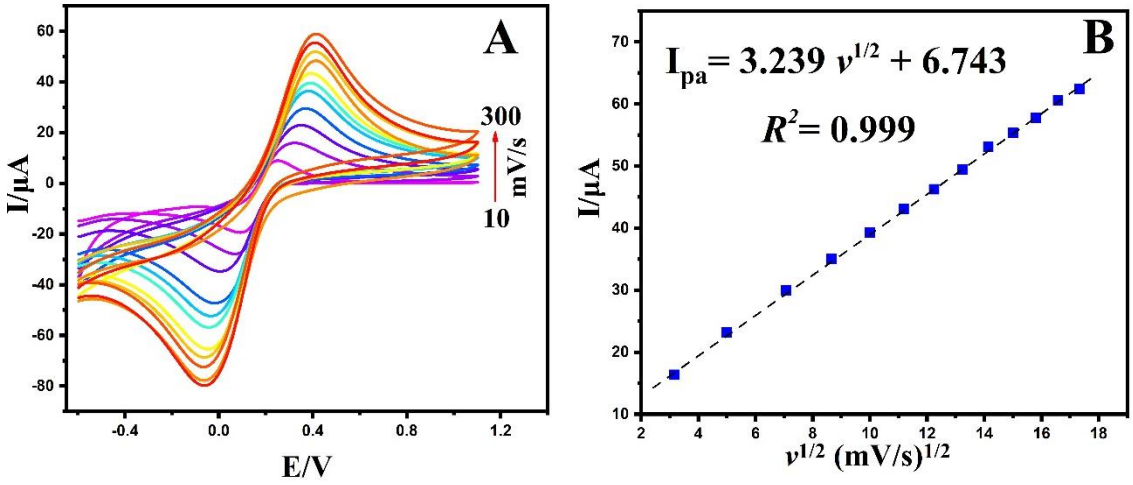

Figure S2. The recorded CV curves at various scan rates in the presence of 5.0 mM $[Fe(CN)_6]^{3-/4-}$ containing 0.1 M KCl (A), and the relationship between Ipa vs. $v^{1/2}$ (B), on bare the GCE.

1.1.Optimization of the MWNTs/GCE preparation conditions

The optimization studies were conducted to maximize the efficacy of the developed electrode in RIBO detection. The initial step involved the critical selection of appropriate buffer solutions, with Britton-Robinson (BR), phosphate buffer saline (PBS), acetate buffer (AC), hydrochloric acid (HCl), potassium chloride (KCl), and sodium hydroxide (NaOH) subjected to thorough examination. Figure S3A illustrates the correlation between the oxidation current and the potential peak of RIBO across various supporting electrolytes. The findings highlight the substantial impact of the presence of 0.01 mM RIBO on both the current and potential peaks. Notably, among the diverse buffers investigated, the BR buffer exhibited the highest current peak, establishing itself as the optimal electrolyte for subsequent investigations into RIBO detection using the devised electrode.

Moreover, the signal of RIBO was investigated at various concentrations of the MWCNTs composite (ranging from 0.2 M to 2.0 M) for the modification of the glassy carbon electrode (GCE). A systematic elevation in the electro-oxidation current of RIBO was noted with the increasing concentration of the MWCNTs composite, as depicted in Figure S3B. However, beyond a composite concentration of 1.0 M, no substantial changes were observed, prompting the identification of 1.0 M as the optimal composite concentration for accurate determination of RIBO.

Furthermore, to optimize the electrode performance, various amounts of MWCNTs (2.0 µL -7.0 µL) were meticulously deposited onto the GCE surface). As illustrated in Figure S3C, elevating the composite quantities up to 5 µL exhibited a noteworthy improvement in the oxidation peak current, signifying an optimal level of MWCNTs incorporation. However, further increments in the amount of MWCNTs dispersion resulted in a noticeable decline in the peak current of RIBO, indicating the critical role of the 5 µL amount in achieving the best electrode response. In pursuit of achieving the utmost determination sensitivity, other pivotal factors, including deposition potential and cumulative time, were diligently investigated. Figure S4A illustrates the impact of different deposition potentials on the peak current of RIBO. Notably, the peak current exhibited a significant increase within the deposition potential range of 0.1 to 1.0 V, followed by a gradual decline within the range of 1.0 to 0.7 V. Hence, 0.7 V was identified as the recommended optimal deposition potential. Furthermore, the influence of deposition time was thoroughly explored within the range of 10 to 200 seconds. As portrayed in Figure S4B, the initial peak current displayed an almost

increase with deposition time until it reached a plateau after 100 seconds. Considering both sensitivity and detection efficiency, an accumulation time of 100 seconds was deemed optimal for further investigations.

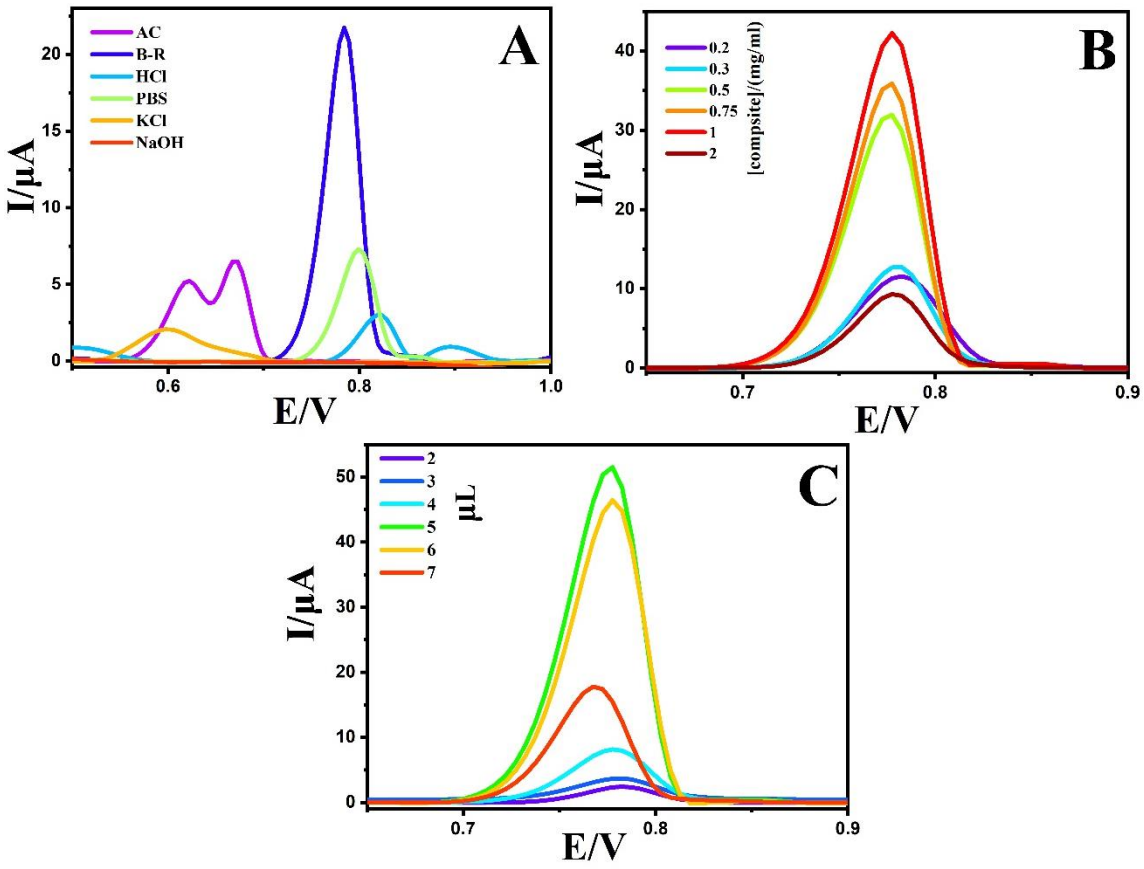

Figure S3. Influence of supporting electrolyte (A), the concentration (B), and the amount (C) of MWCNTs composite on the oxidation peak currents of 0.01 mM RIBO.

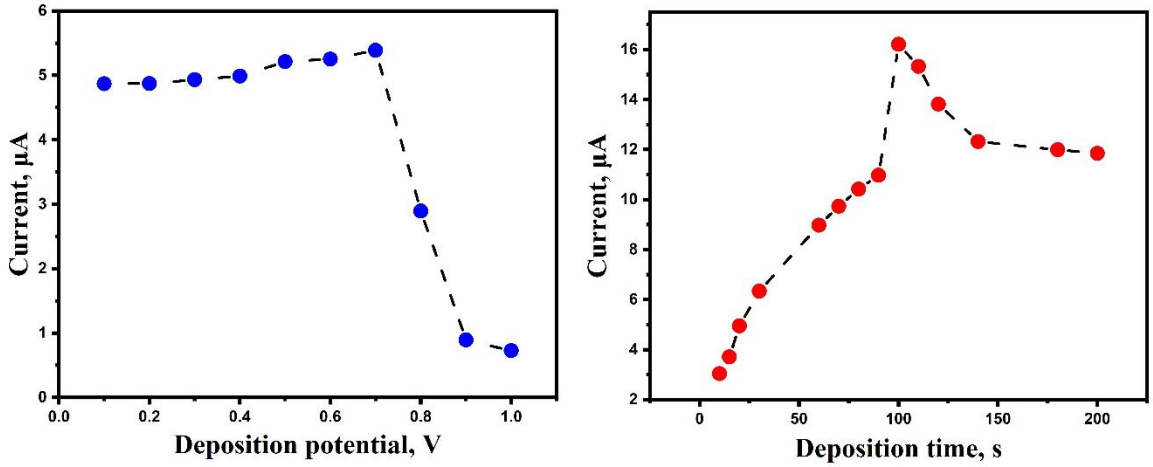

Figure S4. Effect of deposition potential (deposition time: 20s) (A), and effect of deposition time (B); on peak current (deposition potential: 0.7 V) of 0.01 mM RIBO at the MWCNTs /GCE surface.

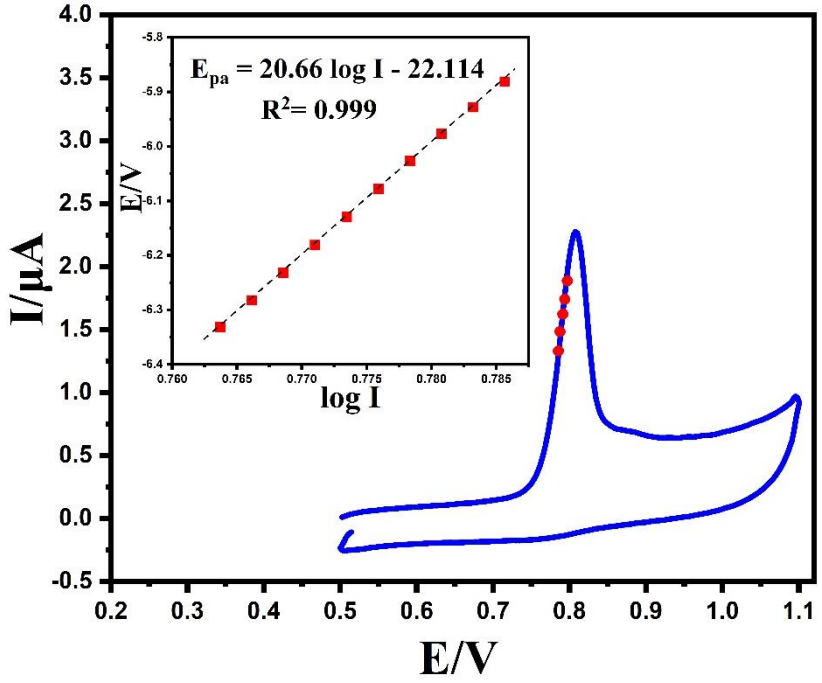

Figure S5. Tafel plot of 0.01 mM RIBO with scan rates of 100 mV s^{-1} at the surface of MWCNTs/GCE.

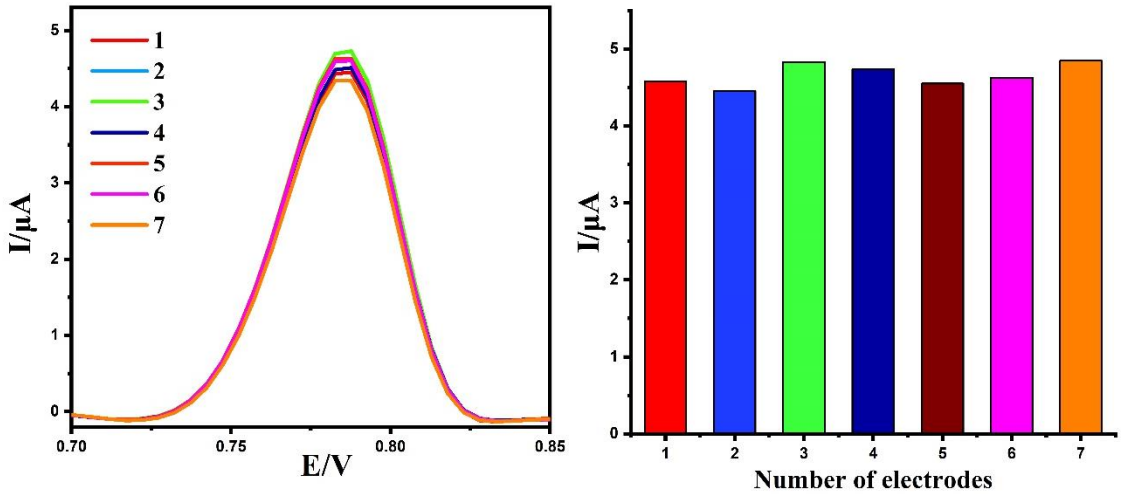

Figure S6. DPVs and histogram of reproducibility of MWCNTs/GCE in 1.0 μM RIBO (BR buffer, pH 2.0).

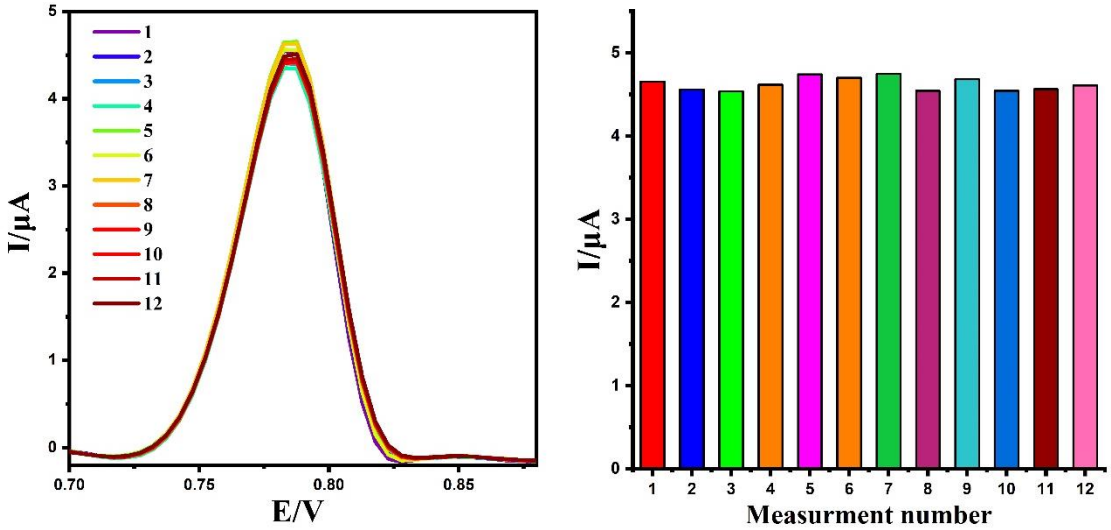

Figure S7. DPVs and histogram of repeatability of MWCNTs/GCE in 1.0 μM RIBO (BR buffer, pH 2.0).

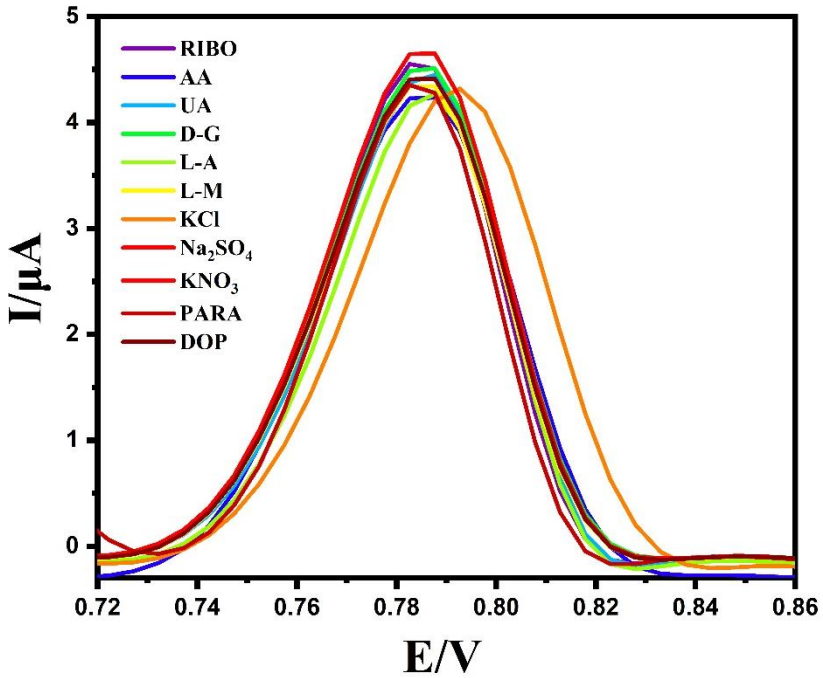

Figure S8. DPVs of selectivity of MWCNTs/GCE in the presence of 1.0 μM RIBO (BR buffer, pH 2.0).